On snow avalanche flow regimes: Inferences from observations and measurements

Peter Gauer[1,2*], Dieter Issler[1,2], Karstein Lied[1], Krister Kristensen[1], and Frode Sandersen[1]

[1]Norwegian Geotechnical Institute, Postboks 3930 Ullevål Stadion, 0806 Oslo, Norway
[2]International Centre for Geohazards, c/o Norwegian Geotechnical Institute, Oslo, Norway

ABSTRACT. Mixed dry-snow avalanches are commonly thought to consist of a dense core and a dilute suspension layer, even though observations and measurements from Canada and Russia have long indicated the presence of an intermediate-density layer ("light flow" or "saltation layer"). We summarize field observations and measurements from Norway and Switzerland, both from spontaneous events and from avalanches released at the test sites Ryggfonn and Vallée de la Sionne. Deposition patterns, high-frequency impact pressure records and radar measurements show that a substantial mass fraction of mixed dry-snow avalanches is flowing in this "fluidized" regime, particularly the head. Based on mechanical considerations, we suggest close correspondence with the grain-inertia regime observed in granular flows; however, the role that the interstitial air plays in avalanches is not clarified at present. Distinguishing between three avalanche flow regimes instead of only two may have important consequences in hazard mapping and the design of protection measures.

Keywords: avalanche dynamics, flow regimes, observations, measurements

1 INTRODUCTION

Recently, The Avalanche Review featured a debate over survival strategies inside different parts (pertaining to different flow regimes) of an avalanche (Birkeland et al., 2008). That discussion may have raised the question for many readers, What do we really know about flow regimes within avalanches? Figure 1 shows the initiation, development, and flow of a so-called mixed dry-snow avalanche. After rapid disintegration of the original slab into small clods and particles, snow grains form a dilute suspension (the "powder cloud") that conceals the flow behavior of the denser parts of the avalanche.

In avalanche dynamics, one traditionally distinguishes between dense-flow avalanches (DFA) and powder-snow avalanches (PSA), but it has been recognized for a long time that dry-snow avalanches often are neither pure DFAs nor pure PSAs. The name mixed-motion avalanches was coined. Mellor (1968) characterizes their dynamical behavior as that of a fluidized solid while Schaerer and Salway (1980) describe a three-layer flow with a so-called "light flow" as a separate entity between and in front of the dense core, underlying the suspension layer. The authors' present understanding fully supports this view; we find the fluidized head often to be significantly faster and more mobile than the dense core, and to be the principal mass source for the suspension layer (Fig. 2). However, some questions persist:

- Do observations and measurements (as Mellor (1968) was asking for) actually support this picture, especially the existence of the (leading) fluidized layer?
- How reliable are these observations and measurements?
- What are the properties of, and mechanisms within, the fluidized layer that can be inferred from the available data?
- Are there alternative interpretations besides a fluidized layer of intermediate density?
- What are the implications for avalanche modeling and hazard mapping?

*Corresponding author's address:
Peter Gauer
Norwegian Geotechnical Institute,
P.O. Box 3930 Ullevål Stadion, 0806 Oslo, Norway
Tel: +47 22 02 31 29; Fax: +47 22 23 04 48; E-mail: pg@ngi.no

Figure 1: Disintegration of an artificially released avalanche in Ophir, Colorado. The avalanche starts as large slabs, but disintegrates rapidly into small clods and particles. Finally, it moves as a mixed dry-snow avalanche with a marked powder cloud. (Snapshots from the video "Out of Ophirica" directed by J. Kuper.)

With these questions in mind, we summarize field observations and measurements from Norway and Switzerland, both from spontaneous events and from avalanches released at the test sites Ryggfonn (RGF) and Vallée de la Sionne (VdlS). For a description of the test sites we refer to (Barbolini and Issler, 2006).

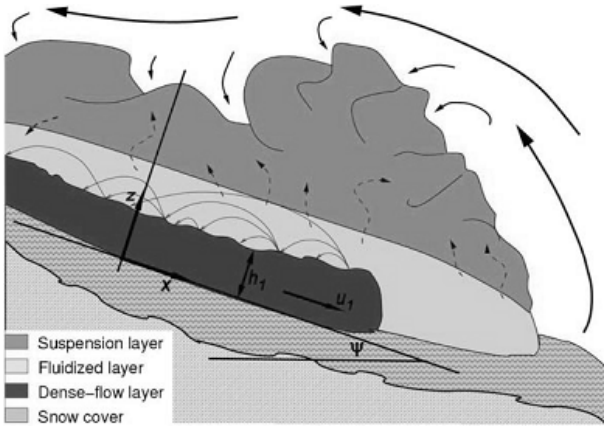

Figure 2: Schematic figure of a dry-snow avalanche showing the dense core, the fluidized (saltation) layer and the powder cloud.

2 FLOW REGIMES

Before we present some of the observations, we start with a brief characterization of the three flow regimes mentioned above to provide some background.

In granular flows an important factor is the particle spacing ratio, L/D, where D is the diameter and L the distance between the midpoints of two particles. For uniformly sized spherical particles, $L/D = (\pi/(6\,c))^{1/3}$ or $c = (\pi/6)(D/L)^3$, with c the volumetric particle concentration. Hence, the particle spacing determines the bulk density of the flowing avalanche, $\rho_b = \rho_a + c(\rho_p - \rho_a)$, where ρ_a and ρ_p are the intrinsic densities of the air and the particles, respectively.

In the frictional or dense-flow regime (Fig. 3a), the particles have persistent contacts with each other or the bed surface, their mean spacing ratio being $L/D \approx 1$. The shear stress is due to the resultant of the integrated normal and tangential (dry friction) forces at the contact points. Stresses are transmitted along preferred directions, so-called force or stress chains.

At sufficiently high shear rates, the pressure from particle collisions drives the particles apart, the network of particle contacts disappears, i. e., the layer becomes fluidized (Fig. 3b). Stresses are primarily transmitted by particle collisions and particle inertia. L/D becomes appreciably larger than 1. To which extent the interstitial air (or the mixture of air and snow grains) contributes to the dynamics is an open question.

The powder cloud or suspension layer (Fig. 3c) behaves like a turbulent flow of a Newtonian fluid. However, turbulence and viscosity depend on the particle concentration. Particle collisions are rare because $L/D \gg 1$. The particle motion is controlled by the

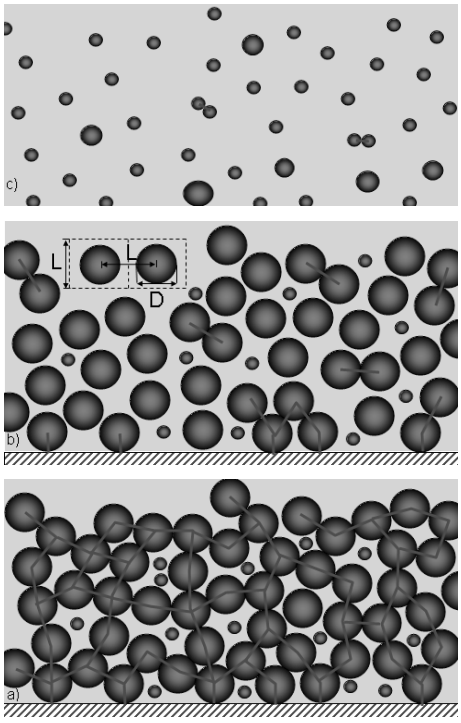

Figure 3: Flow regimes: a) dense flow; b) fluidized flow; c) suspension flow.

fluid forces (drag and lift). The average particle size is smaller than in the fluidized layer or in the dense-flow.

In snow avalanches, particle size is non-uniform and changes over time even inside a layer.

3 OBSERVATIONS AND MEASUREMENTS

One of the certain and frequent observations is that especially the distal part of many dry-snow avalanche deposits has a characteristic texture where a fine-grained matrix embeds particles up to 0.5 m in diameter. The photo sequence in Fig. 1 suggests that many of those particles originate from the initial disintegration of the slide; the time needed for disintegration probably depends on initial snowpack properties like strength and humidity. The trajectories and runout distances of such avalanches indicate increased mobility. The distal deposits most often represent the head of the avalanche, which had the highest speed. The heads of such avalanches are capable of significant erosion (more than 1 m has been observed in many cases) and considerable destruction, as can be seen in Fig. 4. Parts of this avalanche crossed the river Sionne and climbed the opposite slope, whereas a probably slower and more dense part followed the river bed. Destruction of an approximately 15 years old forest reached about 130 m above the river crossing. A

Figure 4: Avalanche event of 1999-02-25 at the Vallée de la Sionne test site, Switzerland (photo P. Gauer).

mature stand at the same location had been taken by a similar event in 1981.

In some cases, the bed surface of the flow can give hints of the flow regime. Figure 5 contrasts the observed bed surfaces of different parts of two mixed-flow avalanches. The first case is due to the dense tail at the end of the deposition zone; the “slickenside” consists of pure ice, indicating sliding motion of a rather compact mass. In the second case, impact craters and abrasion patterns suggest a highly mobile flow dominated by particle impacts. This observation was made higher up in the track in several avalanches, but it was also observed at places further down outside the main gully into which the dense core tends to get channeled (Fig. 6).

Figure 6 shows the erosion pattern of the fluidized head of the 2007-03-22 event. Visual observation of

Figure 5: Sliding surfaces resulting from different flow regimes; left: particle-impact dominated (RGF 2008-04-22); right: sliding tail (RGF 2007-03-22). Photos P. Gauer.

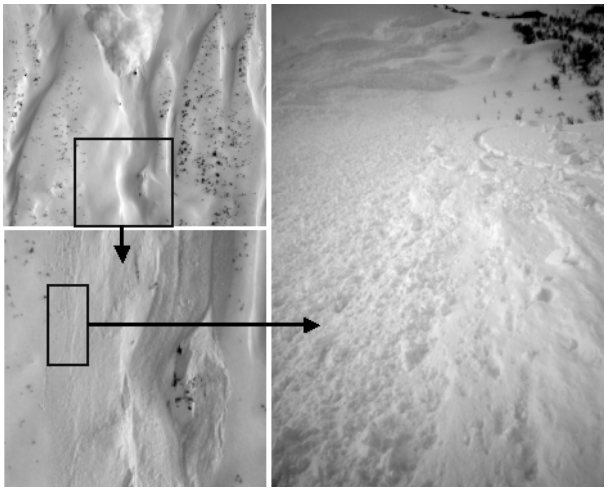

Figure 6: Erosion pattern of a fluidized flow (RGF 2007-03-22). Photos P. Gauer.

the avalanche descent suggested that the fluidized head of this avalanche ran over a small bank whereas the dense tail followed the course of a small creek (as can also be seen in the lower left photo and in Fig. 5). The head eroded about 0.1 m of damp new snow. The right photo shows abrasion traces and impact craters as well as deposited particles with sizes in the range of 0.01–0.1 m, but also some particles of approximately 0.5 m in size.

Measurements of the retarding acceleration in the lower third of the Ryggfonn path also suggest the presence of different flow regimes. Figure 7 plots the mean retarding acceleration, $a_{ret_{LD}}$, for the distance from the midpoint between the steel pylon and the concrete wedge (referred to as LC) and the base of the dam versus the mean front speed between those points, $U_{av} = (U_{LC} + U_b)/2$. The retarding acceleration is defined as

$$a_{ret_{LD}} = \frac{U_b^2 - U_{LC}^2}{2\Delta s} - g \sin \overline{\phi}\,, \qquad (1)$$

where g is the acceleration due to gravity and $\overline{\phi}$ is the mean slope angle of the stretch between LC and the base of the dam. U_b is the velocity at the dam or zero if the avalanche stopped before. Similarly, Δs is the distance between LC and the dam or the distance of the runout measured from LC.

The data represent more than 30 years of measurements at the Ryggfonn site (cf. Gauer and Kristensen, 2005; Norem, 1995, and reports mentioned therein). For the dry-snow avalanches, there is no significant correlation of the retarding acceleration with U_{av}: $a_{ret} = (-4.0 \pm 0.7)\,\mathrm{m\,s^{-2}}$. That holds especially for avalanches that topped or overflowed the dam. This

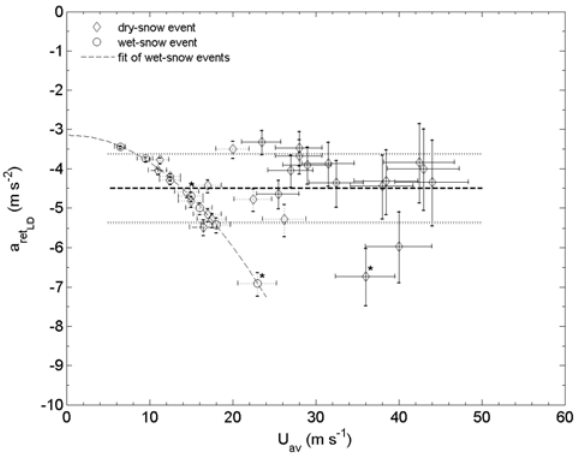

Figure 7: Retarding acceleration, $a_{ret_{LD}}$, between LC and the base of the dam vs. the averaged speed U_{av}. The dashed line shows the mean value and the dotted lines plot plus or minus one standard deviation for all considered events. The full lines in the error bars mark avalanches that overflowed the dam, dotted-lines mark those that stopped at the dam ($\pm$20 m from the top), and dashed lines those that stopped upstream of the dam. Three avalanches that occurred before the dam was built are marked with asterisks.

contrasts strongly with the wet-snow events, which can be fitted well by the parabola $a_{ret_{LD}} = -0.0073\,U_{av}^2 - 3.15\,\mathrm{m\,s^{-2}}$. Incidentally, all dry-snow events with $U_{av} < 20\,\mathrm{m\,s^{-1}}$ also fall on this curve. This is suggestive of two different flow regimes, with the transition occurring at velocities of about 20 m s^{-1} in our case. The overall average is $a_{ret} \approx (-4.5 \pm 0.9)\,\mathrm{m\,s^{-2}}$. For comparison, the retarding acceleration of the front of the VdlS 1999-02-25 avalanche that climbed the opposite slope is estimated as $a_{ret} \approx (-3.2 \pm 2.3)\,\mathrm{m\,s^{-2}}$. Here, we assume a velocity of 60–80 m s^{-1} at the crossing of the river (SLF, 2006) and require a velocity of at least 20 m s^{-1} at the apex to explain the forest destruction. The mean slope angle is about 27°.

Measurements from load plates and pressure cells as well as profiling FMCW radar buried in the ground suggest that different flow regimes are often present within the same dry-same avalanche. Figure 8b is a gray-scale plot of the relative echo intensity vs. distance (vertical axis) and time (horizontal axis). The echo intensity is proportional to the reflectivity at the corresponding point and is thus an indication of the avalanche density (but it also depends on particle size and snow humidity). Fixed-target echo suppression was applied so that only the moving avalanche is depicted. The frontal part of the avalanche (i.e., the first 4 to 5 s) is more dilute than the bottom layer fol-

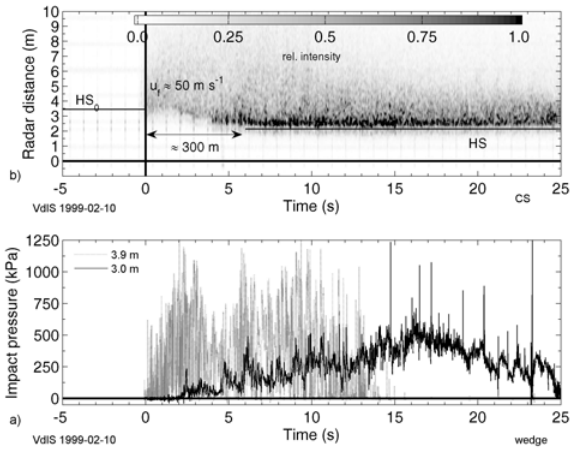

Figure 8: FMCW-radar measurements (top) and corresponding pressure measurements (bottom). (Reference time t = 0 s is taken at arrival at the radar; HS_0 and HS are the estimated snow depths of the original snowpack before and after passage of the avalanche.)

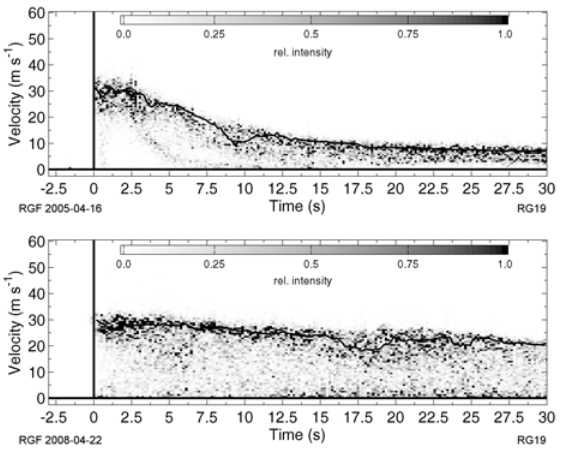

Figure 9: Echo intensity spectra from pulsed Doppler radar measurements. The lines indicate the velocity at maximum echo intensity.

lowing it, which has a thickness of 1–1.5 m. There seems to be a dilute layer riding on top of the dense core. Within the first 5 to 6 s the avalanche eroded the snow to a depth of approximately 1.5 m. Pulsed Doppler radar measurements indicate an avalanche speed of about 50 m s^{-1} at the sensor location during this interval (Gauer et al., 2007b) and thus a length of 200–300 m for the dilute head. Fig. 8a plots corresponding pressure measurements from small, high-frequency load cells for two heights above ground at approximately the same location. The upper load cell shows isolated millisecond impacts of particle or swarms over a low-pressure background, compatible with particle sizes in the distal deposits (Schaer and Issler, 2001); the sensor failed after about 13 s. The lower load cell was most likely buried at the beginning of the avalanche due to deposits of a previous event, and was then eroded free after 3–5 s, which is in accordance with the FMCW radar measurements. It shows a more continuous pressure signal. The striking differences between these signals again indicate differences in composition and flow behavior between the dilute and dense parts. Similar differences could also be recorded at Ryggfonn (Gauer et al., 2007a).

Interpretation of the echo intensity spectra from pulsed Doppler radar is somewhat uncertain due to the lack of comparable data from other sensors. Figure 9 compares the spectra of two artificially released avalanches at Ryggfonn during the first 30 s from arrival at the steel tower (see Barbolini and Issler, 2006, for the site description). The 2005-04-16 event started out as a mixed dry-snow avalanche and probably triggered a second, wet slide (see also Gauer et al., 2008). Hence, the first seconds in the echo intensity plot reflect the motion of a mixed-type avalanche, which then transforms into a more slowly moving wet-snow avalanche. The 2008-04-22 avalanche also started out as mixed type, but in this case the echo intensity spectra suggest higher mobility throughout the interval, and the wider spectra indicate a higher degree of turbulence. This is in accordance with the visual observations.

For the understanding of the fluidized flow regime, reliable measurements of the bulk density of the flowing avalanche are crucial. So far, only indirect, highly uncertain density measurements are available. Table 1 summarizes our current density estimates for the fluidized part. For comparison, assuming a par-

Table 1: Bulk densities of the fluidized layer derived from indirect measurements.

Bulk density (kg m^{-3})	Measurements	Reliability
50–300	observations by Schaerer (cited in Mellor, 1978)	uncertain
20–45 (particle dominated part) 10–150 (matrix)	VdlS 1999 (Schaer and Issler, 2001) load cells ⌀ 0.1 m	large error possible
30–60	VdlS bunker 1999-02-25 (priv. comm. M. Schaer, 1999)	reasonable
50–100	Ryggfonn, large pressure plates (Gauer et al., 2007a)	uncertain

ticle density of about 300–500 kg m^{-3} for typical snow clods (McClung and Schaerer, 1985), the bulk density of a dense flow is at least 150–250 kg m^{-3}. Taking into account that the particle density of the significantly smaller particles in the suspension layer is almost that of ice, and the concentration is probably below 0.01 (or $L/D \geq 3.7$) (Mellor, 1978; Nishimura et al., 1989; Issler, 2003), the bulk density of the powder part is expected to be 10 kg m^{-3} or less.

4 CONCLUSIONS

In the preceding section, we presented avalanche observations and measurements with respect to flow regimes. We find firm evidence for an intermediate flow regime between dense and suspension flow in many dry-snow avalanches, which confirms the observations of Schaerer and Salway (1980). Based on several rough, but independent estimates, the most likely density range of this fluidized regime is 30–100 kg m^{-3}. Direct density measurements would be extremely valuable for removing the remaining uncertainty. We believe that extended parts of fast moving dry-snow avalanche can be fluidized and that the fluidized part in most cases moves ahead of, and farther than, the dense flow. This is in contrast to some of the more traditional model concepts, in which the fluidized or saltation layer rides on top of the dense flow (e.g. Zwinger et al., 2003; Norem, 1991). On the theoretical side there are many unresolved questions, e. g., To which extent can collisions of highly inelastic snow clods sustain fluidization, and which role does the interstitial air play? The internal dynamics of the fluidized layer and its rheology are largely unknown. To sustain fluidization, shear is certainly required. Thus, we expect a non-uniform velocity profile; preliminary measurements (M. Kern, private communication, 2008) seem to confirm this.

Distinguishing between avalanche flow regimes may have important consequences in hazard mapping and the design of countermeasures because the high mobility of the fluidized flow regime allows it to reach areas that cannot be reached by the dense flow (see Fig. 10). However, because the density is two to ten times lower than that of a dense flow, the impact pressure are expected to be considerably less than estimates based on dense-flow models would suggest, yet significantly higher than predicted by pure powder-snow avalanche models.

In addition, pressure measurements imply that the drag factors for avalanches are velocity dependent (Sovilla et al., 2008; Gauer et al., 2008), likely depending on the flow regime; the drag coefficient increases with decreasing velocity, probably due to reduced particle mobility in a dense flow. This is of importance in the planning and construction of mast-like structures in avalanche prone areas. In order to account for flow regime transitions in avalanche models for hazard mapping, a density-dependent rheological model is required. A first step in this direction was presented in an exploratory study by Issler and Gauer (2008).

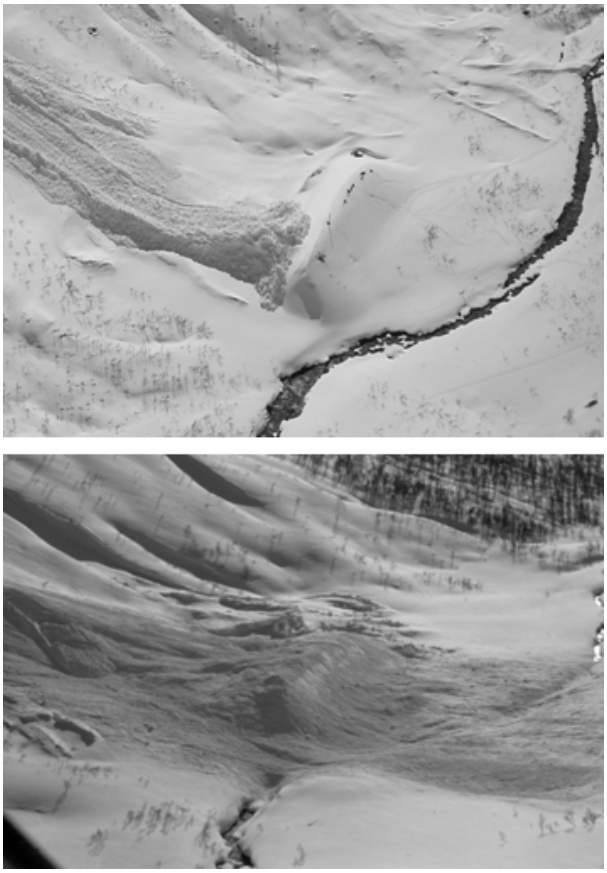

Figure 10: Deposition of the wet-snow part of the 2005-04-16 avalanche (top; snapshot from video by K. Kristensen) and of the dry-snow avalanche 1997-02-08 (bottom; photo NGI).

ACKNOWLEDGMENTS

This work was funded through NGI's SIP-program "Avalanche research". SLF provided access to FMCW-radar and pressure data from the VdlS 1999-02-10 event. This is publication no. 209 from the International Centre for Geohazards.

REFERENCES

Barbolini, M. and D. Issler, 2006: Avalanche Test Sites and Research Equipment in Europe: An Updated Overview. Final-Report Deliverable D8, SATSIE Avalanche Studies and Model Validation in Europe.

Birkeland, K., P. Bartelt, and T. Meiners, 2008: Avalanche survival strategies for different parts of a flowing avalanche: Merging theory and practice to increase your odds. *The Avalanche Review*, **26**, 12.

Gauer, P., D. Issler, K. Lied, K. Kristensen, H. Iwe, E. Lied, L. Rammer, and H. Schreiber, 2007a: On full-scale avalanche measurements at the Ryggfonn test site, Norway. *Cold Regions Science and Technology*, **49**, 39–53, doi:10.1016/j.coldregions.2006.09.010.

Gauer, P., M. Kern, K. Kristensen, K. Lied, L. Rammer, and H. Schreiber, 2007b: On pulsed Doppler radar measurements of avalanches and their implication to avalanche dynamics. *Cold Regions Science and Technology*, **50**, 55–71, doi:10.1016/j.coldregions.2007.03.009.

Gauer, P. and K. Kristensen, 2005: Avalanche Studies and Model Validation in Europe, SATSIE; Ryggfonn measurements: Overview and dam interaction. NGI Report 20021048-10, Norwegian Geotechnical Institute, Sognsveien 72, N-0806 Oslo.

Gauer, P., K. Lied, and K. Kristensen, 2008: On avalanche measurements at the norwegian full-scale test-site ryggfonn. *Cold Regions Science and Technology*, **51**, 138–155, doi:10.1016/j.coldregions.2007.05.005.

Issler, D., 2003: Experimental information on the dynamics of dry-snow avalanches. *Dynamic Response of Granular Materials under Large and Catastrophic Deformations*, K. Hutter and N. Kirchner, eds., Springer, volume 11 of *Lecture Notes in Applied and Computational Mechanics*, 109–160.

Issler, D. and P. Gauer, 2008: Exploring the significance of the fluidised flow regime for avalanche hazard mapping. *Annals of Glaciology*, **49**, in press.

McClung, D. M. and P. A. Schaerer, 1985: Characteristics of flowing snow and avalanche impact pressures. *Annals of Glaciology*, **6**, 9–14.

Mellor, M., 1968: Cold Regions Science and Engineering. Part III: Engineering, Section A3: Snow Technology, Avalanches, Cold Regions Research & Engineering Laboratory, Hanover, New Hampshire.

— 1978: *Dynamics of snow avalanches*, Elsevier Sci Ltd, New York, chapter 23. 753–792.

Nishimura, K., H. Narita, N. Maeno, and K. Kawada, 1989: The internal structure of powder-snow avalanches. *Annals of Glaciology*, **13**, 207–210.

Norem, H., 1991: Estimating snow avalanche impact pressures on towers. *Proceedings of a Workshop on Avalanche Dynamics, 14–19 May 1990*, H. Gubler, ed., Mitt. Eidgenöss. Inst. Schnee- Lawinenforsch. Nr. 48, 42–56.

— 1995: The Ryggfonn Project: Summary Report 1981–1995. Techreport A952-1, Dr. ing. Harald Norem A/S Consultant in Snow Engineering, Molde, Norway.

Schaer, M. and D. Issler, 2001: Particle densities, velocities and size distributions in large avalanches from impact-sensor measurements. *Annals of Glaciology*, **32**, 321–327.

Schaerer, P. A. and A. A. Salway, 1980: Seismic and impact-pressure monitoring of flowing avalanches. *Journal of Glaciology*, **26**, 179–187.

SLF, 2006: Vallée de la Sionne 1998/99. Schlussbericht, Swiss Federal Institute for Snow and Avalanche Research.

Sovilla, B., M. Schaer, M. Kern, and P. Bartelt, 2008: Impact pressures and flow regimes in dense snow avalanches observed at the Vallée de la Sionne test site. *Journal of Geophysical Research, Earth-Surfaces*, **113**, F01010, doi:10.1029/2006JF000688.

Zwinger, T., A. Kluwick, and P. Sampl, 2003: Numerical simulation of dry-snow avalanche flow over natural terrain. *Dynamic Response of Granular Materials under Large and Catastrophic Deformations*, K. Hutter and N. Kirchner, eds., Springer, volume 11 of *Lecture Notes in Applied and Computational Mechanics*, 109–160.